

Review

# Morphology and Photocatalytic Activity of Zinc Oxide Reinforced Polymer Composites: A Mini Review

Mokgaotsa Jonas Mochane <sup>1,\*</sup>, Mary Tholwana Motloulung <sup>1</sup>, Teboho Clement Mokhena <sup>2</sup>  
and Tladi Gideon Mofokeng <sup>3</sup>

<sup>1</sup> Department of Life Sciences, Central University of Technology, Free State, Private Bag X20539, Bloemfontein 9301, South Africa

<sup>2</sup> Advanced Materials Division, Nanotechnology Innovation Center (NIC), Randburg 2194, South Africa

<sup>3</sup> Center for Nanostructures and Advanced Materials, DSI-CSIR Nanotechnology Innovation Center, Council for Scientific and Industrial Research, Pretoria 0001, South Africa

\* Correspondence: [mochane.jonas@gmail.com](mailto:mochane.jonas@gmail.com)

**Abstract:** There is an approximately 3% of fresh water available globally for utilization, while the rest of the water is not available for usage, leaving billions of people with less water. Less water availability means that the majority of water consists of pollutants either in ground water or drinking water, which in turn may have a negative impact on the environment and people. Various methods such as plasma technology, flocculation, neutralization, and disinfection have been utilized for wastewater treatment. The wastewater treatment methods have been found to be selective in terms of the removal of other pollutants, as a result, the majority of them are unable to remove pollutants such as antibiotics at a trace level. In order to ensure that there is a complete removal of pollutants from water, there is a need for the development of alternative wastewater treatment methods. The use of solar light by photocatalysis is an alternative method for the degradation of toxic pollutants. Different photocatalysts such as zinc oxide (ZnO), titanium dioxide (TiO<sub>2</sub>), and silver (Ag) have been used in the process of photocatalysis. However, the above photocatalysts were found to have drawbacks such as agglomeration at higher contents and health problems during transportation. To solve the above problem, the nanoparticles were immobilized in various matrices such as polymers and ceramics, with polymers being preferred because of low cost, chemical inertness, and high durability. The current review discusses various methods for the preparation of ZnO and its synergy with other nanoparticles incorporated in various polymer matrices. Because it is known that the preparation method(s) affects the morphology, the morphology and the photocatalytic activity of various ZnO/polymer composites and hybrid systems of ZnO/other nanoparticles/polymer composites are discussed in depth.

**Keywords:** photocatalysis; pollutants; irradiation; wastewater; photocatalyst



**Citation:** Mochane, M.J.; Motloulung, M.T.; Mokhena, T.C.; Mofokeng, T.G. Morphology and Photocatalytic Activity of Zinc Oxide Reinforced Polymer Composites: A Mini Review. *Catalysts* **2022**, *12*, 1439. <https://doi.org/10.3390/catal12111439>

Academic Editors: Victorio Cadierno and Raffaella Mancuso

Received: 29 September 2022

Accepted: 9 November 2022

Published: 15 November 2022

**Publisher's Note:** MDPI stays neutral with regard to jurisdictional claims in published maps and institutional affiliations.



**Copyright:** © 2022 by the authors. Licensee MDPI, Basel, Switzerland. This article is an open access article distributed under the terms and conditions of the Creative Commons Attribution (CC BY) license (<https://creativecommons.org/licenses/by/4.0/>).

## 1. Introduction

The current generation is having serious problems when it comes to the energy crisis and pollution [1–5]. More people have died due to pollution every year when compared to war or violence. According to the World Health Organization, there are approximately 250 million people who die every year due to diseases resulting from contaminated natural sources such as cholera, typhoid fever, polio, etc. [6].

Water pollution has been the major concern for researchers globally since it is associated with deadly diseases. Water pollution is caused by various sources such as the industrial and agricultural sectors [7]. The industrial sector is leading in terms of water pollution as various industries such as the leather, textile, food, printing, and pharmaceutical release wastewater into the environment [7]. Wastewater released by the industries consists mainly of dangerous pollutants in the form of organic and inorganic pollutants. There is a need for the utilization of environmentally friendly methods in order to reduce pollution as it is associated with dangerous diseases. There are different experimental methods that

have been employed to reduce pollution, not all of it, however, they have contributed significantly in terms of the reduction in pollution. For example, methods such as membrane adsorption [8], chemical coagulation [9], adsorption techniques [10], sedimentation [11], flocculation [12], and photocatalysis [13] have been used for the removal of various pollutants. One of the most preferred methods in terms of reducing pollution is the utilization of the technique known as photo-catalysis. Except for photocatalysis, these techniques were found to have limitations with regard to the removal of pollutants, especially the dyes from an aqueous medium. Photocatalysis is the preferred method over other methods due to (i) the conversion of pollutants into less toxic products; (ii) advanced oxidation may result in non-selectivity of pollutants; and (iii) less possibility of forming hazardous materials as by-products [14–18]. Various nanoparticles have been used as photocatalysts, which include titanium dioxide ( $\text{TiO}_2$ ) [14,15], stannic oxide ( $\text{SnO}_2$ ) [16], ZnO [17], silver, and ferric oxide ( $\text{Fe}_2\text{O}_3$ ) [18]. Amongst the above-mentioned nanoparticles, the most commonly utilized nanoparticles for photocatalysis are ZnO,  $\text{TiO}_2$ , and silver. Figure 1 illustrates the number of publications in the photocatalysis of the three nanoparticles. According to Figure 1, in 2018 and 2019,  $\text{TiO}_2$  was found to be the leading nanoparticle with second place taken by silver (Ag) in terms of the photocatalytic activity research. However, there was a steady increase in the number of publications for ZnO in 2021 and 2022 when compared to both  $\text{TiO}_2$  and Ag. The driving force behind this paradigm shift results from the above-mentioned merits associated with ZnO. Figure 2 illustrates the top countries in terms of the research on the photocatalysis of ZnO.

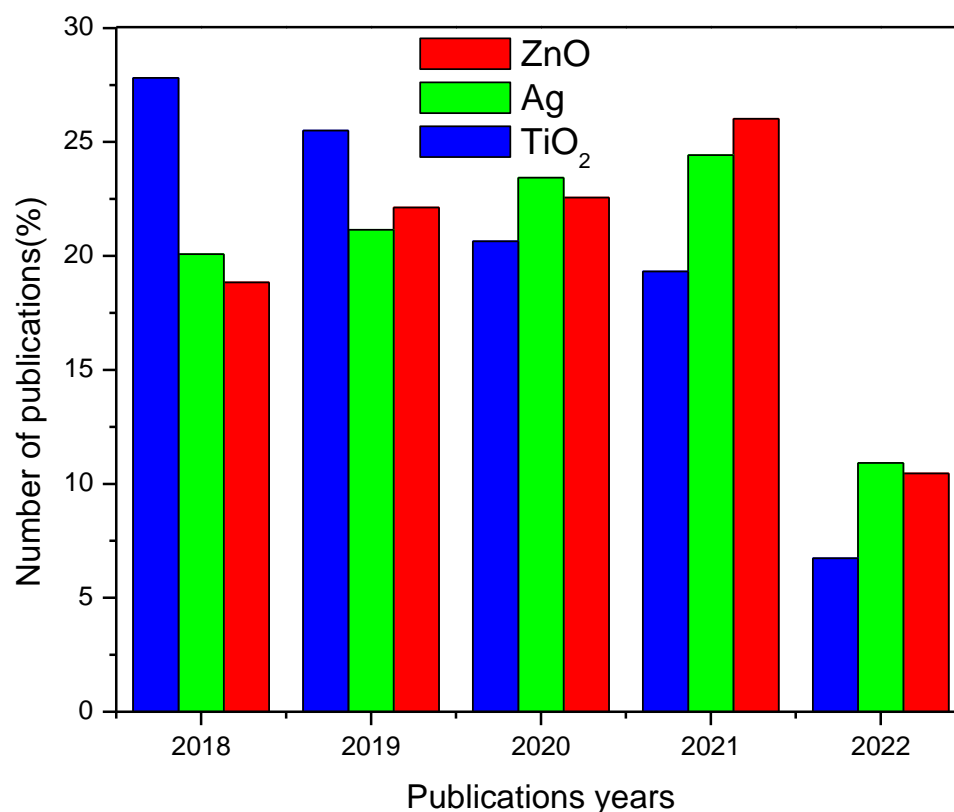


**Figure 1.** Number of publications on photocatalytic activity of ZnO, Ag, and  $\text{TiO}_2$  from 2018 to 2022. As of 7 July 2022.

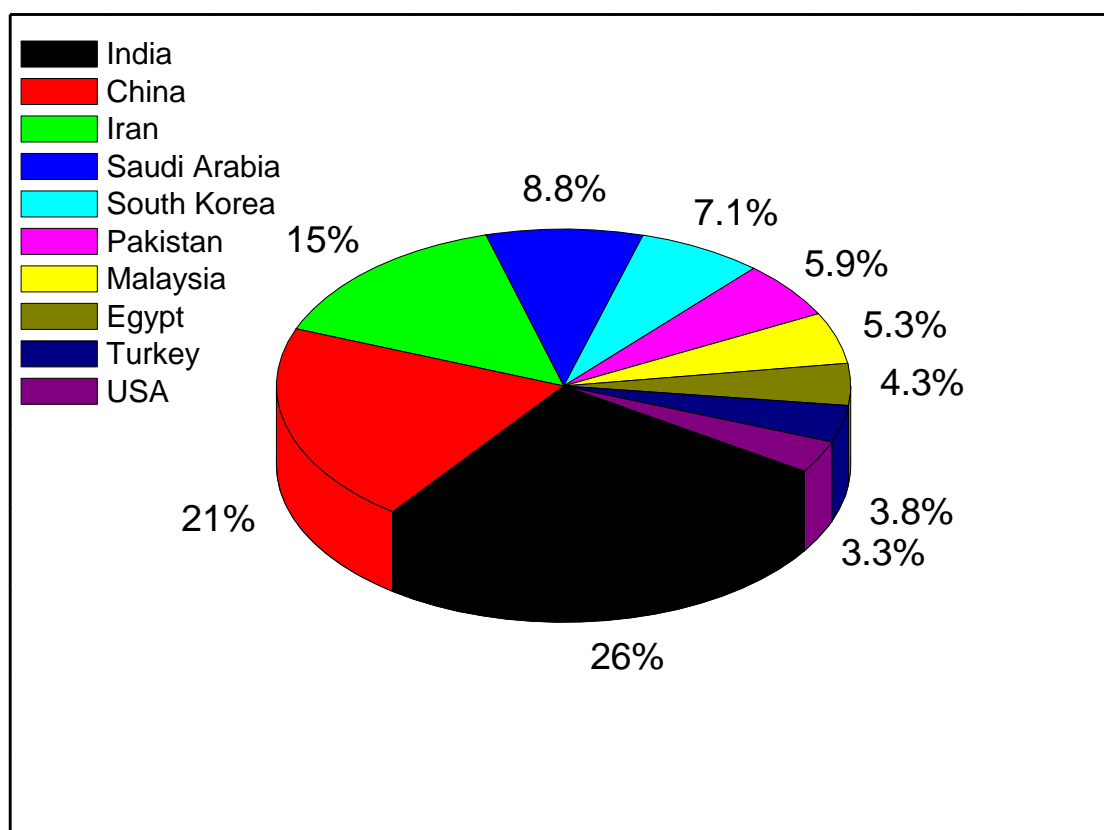


**Figure 2.** Leading countries in the study of photocatalysis for ZnO. As of 7 July 2022.

Various countries have taken the lead in terms of the photocatalytic activity of ZnO (Figure 3). For example, India is the leading country in terms of the ZnO photocatalysis. The main reason why India is leading in terms of the photocatalysis of ZnO is because of the need to clean their wastewater to accommodate their high population needs. The pressure comes from their population, which is estimated to reach ~1.5 billion by 2050, with the projection that 50% of the total population is expected to be in urban areas [19]. An increase in urbanization will trigger more water usage, as a result, the need for the treatment of wastewater. There are other reasons as to why ZnO nanoparticles are favored over others. For example, ZnO has been chosen because of its wide band (*viz.* 3.37 eV) and large excitation binding energy (approximately 60 meV). Furthermore, the various morphologies associated with ZnO such as nanorods, nanotubes, and nanowires are also key for the utilization of ZnO in photocatalysis [20–24]. Aside from the photocatalytic efficacy of ZnO-based materials, their long-term effect on the environment/health and cost associated with their recovery and reusability have been of major concern. The incorporation of these materials into polymers overcomes these limitations. The immobilized ZnO onto polymeric materials offers the possibility for their recovery and reuse in wastewater treatment, hence reducing the costs. This review paper discusses the photocatalytic activity of zinc oxide incorporated in various polymer matrices. Furthermore, the synergistic effect of ZnO with other nanoparticles is also reported with regard to photocatalytic activity.

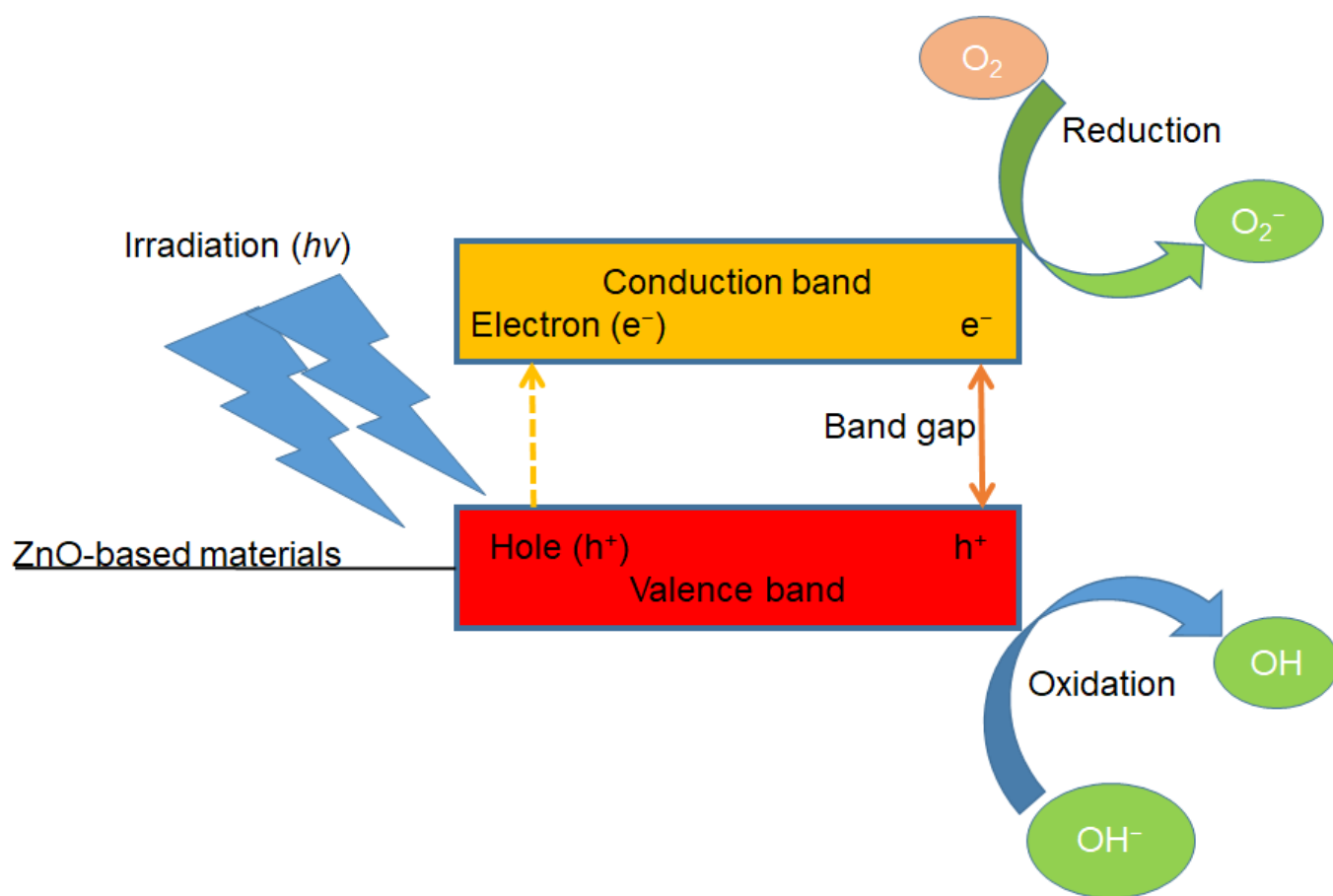


**Figure 3.** A schematic representation of the photocatalytic mechanism.

## 2. The Mechanism of Photocatalytic Activity

It is known that organic pollutants, especially the colored (*viz.* dyes) ones, have a tendency of being fully dissolved in water. It is well-documented that during the process of dye coating, almost 20% of the dye is lost, and it is transferred directly into the environment [25]. The presence of organic pollutants in the environment has the following disadvantages in the environment and health at large: (i) they have a negative impact on the marine life; (ii) they cause significant ecological problems; and (iii) pose serious health complications [26]. To overcome the above problems caused by organic pollutants, the utilization of the photocatalysts provide a better solution, as explained in the Introduction section. Photocatalytic activity occurs when a semiconductor nanoparticle absorbs a photon that has an energy equal to or more than the band gap of the nanoparticle. The irradiation of the photocatalyst with a corresponding wavelength transfers the electrons from the valence band to the conduction band and therefore, equal electron-hole pairs are formed. The excited electrons advance in a single electron reduction, and together with the  $O_2$ , forms superoxide radicals. A reaction between electron holes and water produces the hydroxyl radicals. The produced radicals (i.e., superoxide and hydroxyl radical) are highly reactive and leads to the degradation of the organic pollutants to less toxic products [27]. It is worth mentioning that the resulting superoxide radicals are essential for metal ion reduction, and thus serve as important radicals in wastewater treatment. Figure 3 provide a detailed photocatalytic mechanism.

## 3. The History and Origins of Photocatalysis with Regard to $TiO_2$ , ZnO, and Ag

According to the CAPLUS and MEDLINE database (Sci Finder), the concept of photocatalysis was first introduced between 1910 and 1920 [28]. However, Teichner [29] emphasized that the research, more especially, the reactions based on the photocatalytic

concept, began 52 years ago.  $\text{TiO}_2$  was utilized earlier than 1970 in various applications that are more related to its photocatalytic applications. For example, in 1929, Keidel et al. [30] reported on the degradation of the paints and fabrics that were coated with  $\text{TiO}_2$ . In 1938,  $\text{TiO}_2$  was utilized as a photosensitizer to photobleach the dyes, which occurred in the presence of oxygen and produced reactive oxygen species [31]. It was observed from the UV absorption that the produced reactive oxygen species eventually caused the bleaching of the dyes. In 1956, Kato and Mashio [32] reported on the auto-oxidation by  $\text{TiO}_2$ , which was utilized as a photocatalyst. In this study,  $\text{TiO}_2$  was added into solvents and the mixture was analyzed by UV irradiation. The results were such that there was an auto-oxidation of the solvents while there was the formation of hydrogen peroxide in the process. In 1972, Fujishima and Honda [33] reported on the electrochemical photolysis of water at the semiconductor electrode. The authors designed an electrochemical cell whereby the  $\text{TiO}_2$  electrode was connected with the platinum black electrode via an external load. The irradiation of the  $\text{TiO}_2$  electrode followed the current from the platinum electrode to the  $\text{TiO}_2$  one via an external circuit. The authors concluded that the direction of the current showed that the oxidation reaction took place at the  $\text{TiO}_2$  electrode and reduction occurred at the platinum black electrode. The authors concluded that the water may have been decomposed by visible light into both oxygen and hydrogen in the absence of any external voltage. Despite the studies above, a real breakthrough in the research of  $\text{TiO}_2$  photocatalysis was conducted in the early 1960s under UV irradiation [14]. The first research paper that might be considered as the first one on the photocatalysis of  $\text{TiO}_2$  under UV light was reported by Kato and co-workers in 1964 [34]. This study reported on the liquid phase oxidation of the tetralin by employing titanium oxide as the catalyst. Generally, the authors reported that the photocatalytic activity of the system was different, depending on various factors such as the type of titanium oxide used, surface area, and lattice defects. After the investigation of the above study by Kato et al., various authors began reporting on  $\text{TiO}_2$  as a catalyst in photocatalytic reactions by using UV irradiation [35–45]. Despite  $\text{TiO}_2$  being utilized in the past as a catalyst in photocatalysis,  $\text{ZnO}$  nanoparticles have shown a huge potential as an alternative catalyst to  $\text{TiO}_2$  for photocatalysis. Generally, zinc oxide has been studied by scientists since the 1930s [42]. Naturally, zinc oxide is found as an oxidic material in mineral zincite in the hexagonal wurtzite structure and was discovered in 1810 before being synthesized in Europe in 1850. The mineral zincite is found in various countries such as USA (New Jersey), Italy (Tuscany), Namibia, Poland, Spain, and Australia [42]. The first applications of zinc oxide included in watercolors as well as a diluent in paints, while in the late 1890s, it was used for the fabrication of oil paints. Currently, the scientific community has emphasized  $\text{ZnO}$  as a semiconductor. The first piezoelectric properties of  $\text{ZnO}$  were discovered in 1960, which led to the first electronic applications of  $\text{ZnO}$  as a thin layer in a surface sound wave [42]. The first report on silver nanoparticles was conducted by M.C. Lea 133 years ago, which involved the synthesis of the citrate stabilized silver in the form of a colloid, with an average diameter in the range of 7–9 nm [43]. Furthermore, in 1902, there was a study that reported on the stabilization of silver by employing the proteins [44]. The study was conducted in 1902, however, this type of nano silver has been in existence since 1897 under the name “Collargol”. Collargol was mostly used in medical applications, and it was found to have a diameter of 10 nm. After the discovery of silver nanoparticles, as briefly discussed above, more studies over the next decade have reported on silver nanoparticles. For example, in 1953, a patent was published by Moudry [45] about gelatin silver nanoparticles, which were reported to have a diameter of 2–20 nm. Nowadays, the most common utilization of these three nanoparticles (*viz.*  $\text{TiO}_2$ ,  $\text{ZnO}$  and Ag) is in photocatalysis.

#### 4. Photocatalytic Activity of $\text{ZnO}$ Reinforced Polymer Matrices

In this section, the preparation method, morphology, and photocatalytic activity of the  $\text{ZnO}$ /polymer composites are discussed. Furthermore, the morphology and photocatalytic activity of  $\text{ZnO}$  and its synergy with other nanoparticles incorporated in various polymer

matrices is discussed. There is also a brief discussion on the properties of the two systems (*viz.* ZnO/polymer and ZnO/other nanoparticles/polymer composites) after the exposure to UV irradiation.

#### 4.1. ZnO Reinforced Polymer Composites: Preparation, Morphology, and Photocatalytic Activity

A fair number of studies have investigated the photocatalytic activity of the polymer/ZnO composites [46–51]. Factors such as the type of ZnO nanoparticle, modification of the nanoparticle, type of pollutant (i.e., dyes, etc.), irradiation time, synergy of the nanoparticles, and type of the polymer utilized for the photocatalysis applications of the polymer nanocomposite were found to affect the photocatalytic activity. Qiu et al. [46] reported on the photocatalytic removal of three unwanted materials in the form of phenol, methyl orange, and rhodamine B by fabricating ZnO/poly-(fluorene-*co*-thiophene) (PFT). The nanocomposites were fabricated by the following steps: PFT was dissolved in the tetrahydrofuran (THF) for 1 h. Furthermore, 0.5 g of ZnO powder was dissolved in ethanol solution and the mixture was stirred for 120 min. The composite was formed by adding PTF solution into a ZnO suspension through stirring. To ensure a uniform dispersion, the PTF/ZnO composites were further stirred for 30 min. Generally, it is important in photocatalytic activity to have a better dispersion of the nanoparticle as this enhances the chances of getting positive results. The SEM images in the absence of PTF showed that the particle size of ZnO did not change in the presence of PTF (Figure 4). The advantage of utilizing PTF in this system is that PTF is a good photosensitizer. The statement is supported by the fact that approximately 40% of the phenol was removed in the PTF/ZnO system when compared with 10% removal with neat ZnO alone. The photocatalytic removal of the dyes (i.e., rhodamine B and methyl orange) were also reported in the absence of light (experiment taking place in the dark). The two types of dyes were found to undergo different photocatalytic removal. For example, in the case of rhodamine B, for the PTF/ZnO system, there was a reduction in the absorption peak, which was accompanied by hypsochromic shifting, with the shifting associated with the dismantling of the dye chromogen. However, methylene blue showed a different behavior—there was still a reduction in the absorption peak, but there was no shifting in the hypsochromic form.

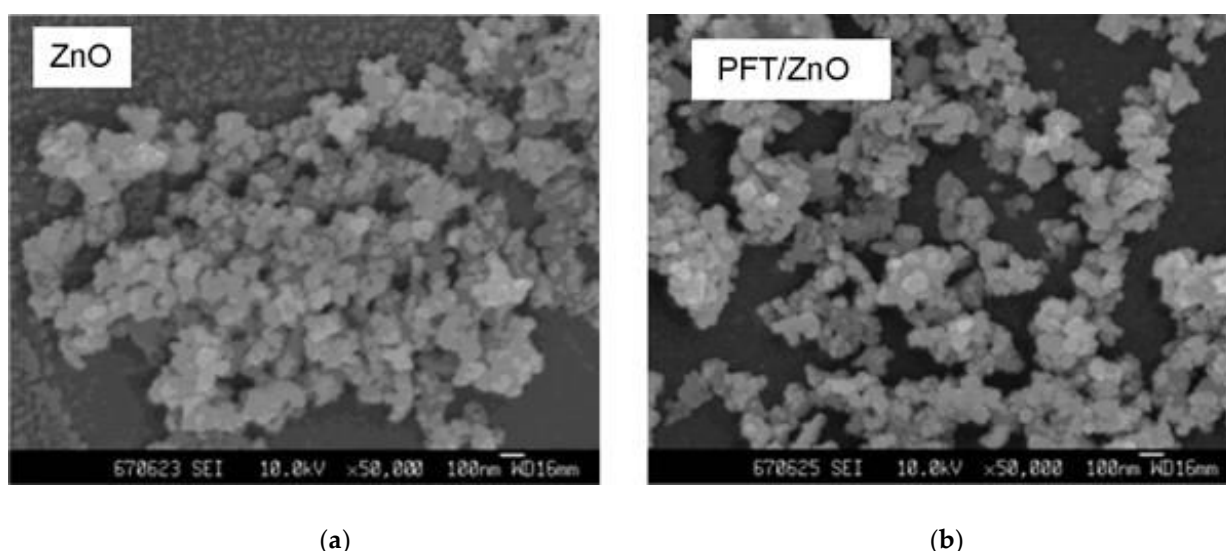


**Figure 4.** TEM images of the (a) ZnO and PFT/ZnO (b). (Reprinted with permission from Ref. [46], ©Elsevier 2008).

Prasert et al. [48] reported on the various properties of the polypropylene/ZnO nanocomposites including the photocatalytic dye degradation. The composites were fabricated with a twin-screw extruder, with 0, 0.5, 1, and 2 wt% of ZnO. The ZnO nanoparticles was reported to have an average diameter of  $72 \pm 18$  nm. There was a good dispersion of

the ZnO nanoparticles into the PP matrix (Figure 5). White spots circled in red represent the ZnO particles well dispersed within the host polymeric material with size less than 100 nm (Figure 5d).

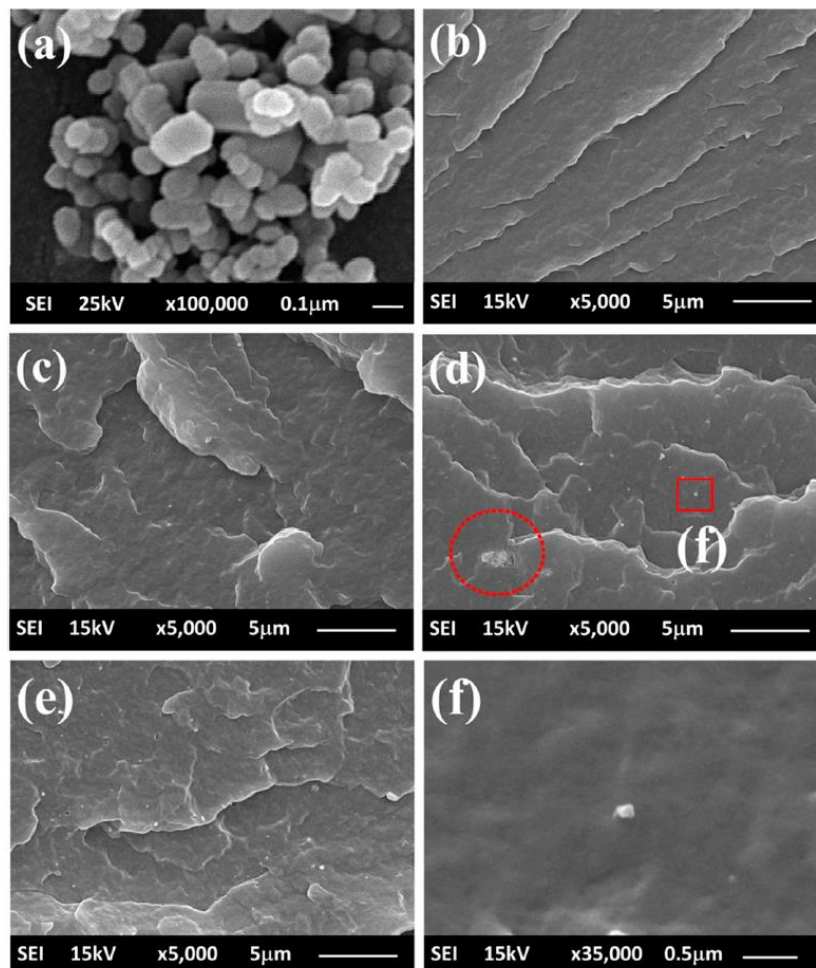


**Figure 5.** SEM images of the (a) neat ZnO nanoparticles and (b–e) represent the PP/ZnO nanocomposites whereas (f) inset of (d). Reprinted from [48].

The photocatalytic activity test was conducted through the degradation of methylene blue (MB) in UV irradiation [48]. PP containing 0.5% and 1% ZnO displayed MB degradation ranging in between 15 and 20% within 5 h, whereas the inclusion of 2% led to 59% degradation within 5 h. This is because of the limited number of ZnO exposed on the surface of PP, *viz.* at higher ZnO content, more of these fillers protrude on the surface of the host polymer and hence higher MB degradation is achieved (Figure 6). The photostability and reusability of the composites for MB degradation were carried out three times. It was noticed that the nanocomposites maintained a MB degradation efficiency of ~59% for three cycles. It can be deduced that the use of melt-mixing has to be carefully considered in order to control the number of ZnO particles being exposed to the dyed solution. Therefore, large quantities of ZnO are required to achieve a reasonable degradation efficacy because most of these fillers are embedded within the host polymeric material.

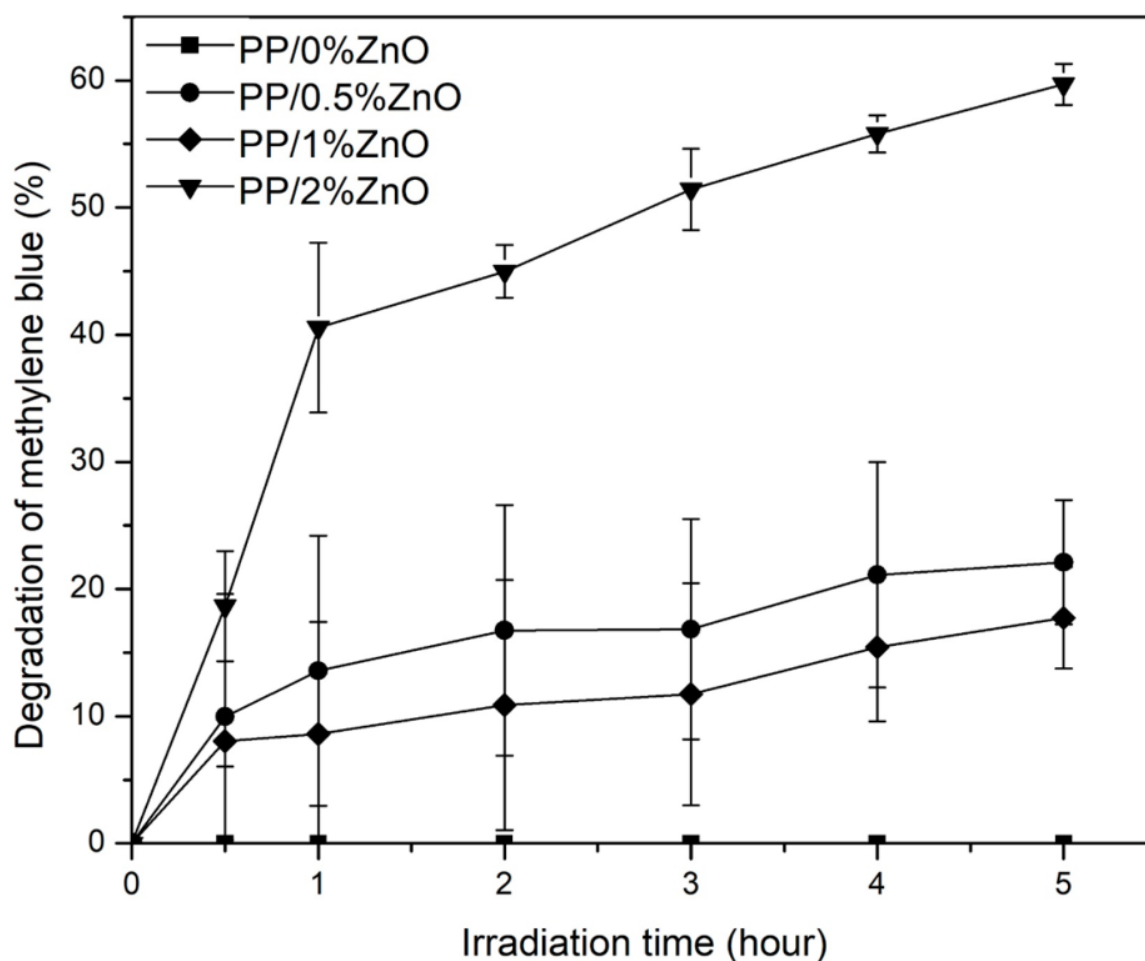


**Figure 6.** Photocatalytic degradation of methylene blue by using PP/ZnO nanocomposites as a catalyst. Reprinted from [48].

Coating and growing particles on the surface of the polymers have been reported as an alternative method to ensure that there is a sufficient number of ZnO particles exposed on the surface of the polymer. For instance, Colmenares et al. reported [50] on the photocatalytic activity of ZnO nanorods incorporated into a polypropylene (PP) nonwoven fiber mat. The samples were prepared by three steps: (i) plasma treatment of PP polymer; (ii) discharge of ZnO into the PP fibers; and (iii) hydrothermal growth of the ZnO rods. Plasma treatment is very important since it enhances the coating of fibers with ZnO, and as a result, enhances the uniform dispersion of the nanoparticles. The uniform dispersion of the nanoparticle may result in high activity as well as stability during the photocatalytic activity of phenol. The fabricated samples were used for photocatalytic degradation of the aqueous phenol. The photocatalytic test was investigated for neat PP, PP/ZnO, and commercial ZnO. Figure 7 illustrates a typical photocatalytic reaction system employed in this study. The ZnO/PP system was found to be 3-fold higher than commercial ZnO in relation to the photocatalytic degradation of phenol. There are a few reasons associated with such an enhancement in the system consisting of ZnO/PP, first, this is due to the presence of 1D ZnO nanorods, which provides a vertical array structure with a lot of active sites and is able to collect light. Second, there is an ease of photo-electron flow to PP and resistance of the recombination of both the holes and the electrons.

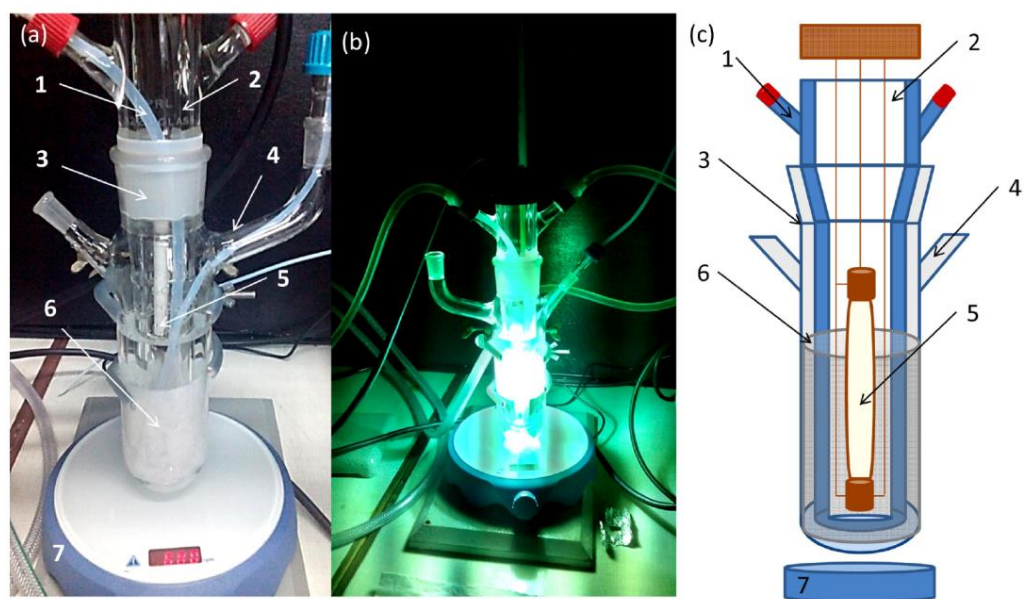


**Figure 7.** Photocatalytic system. (a) Before the reaction, (b) during the reaction, and (c) schematic representation. (1) lamp cooling system (2) double-walled immersion well (3) photoreactor (4) port for taking samples (5) 125 W UV lamp (6) photocatalyst (7) magnetic stirrer. (Reprinted with permission from Ref. [50]. © Elsevier 2015).

A wide variety of conductive polymers including polyaniline (PANI), polythiophene, and polypyrrole have been employed to improve the photocatalytic efficiency of inorganic semi-conductors for various pollutants [49]. These polymers have extended  $\pi$ -bonding that contribute to their conductivity. In general, the combination of the fillers and conductive polymers resulted in higher photocatalytic activity when compared to fillers alone [52–54]. Asgari et al. [49] reported on the preparation of PANI/ZnO via aniline in situ polymerization for the photodegradation of a metronidazole (MNZ) synthetic antibacterial agent. The pH of the solution was found to be one of the factors playing a key role in the removal of unwanted materials. The pH of the solution is key in terms of examining the influential radicals in the oxidation process [49]. The effect of pH of the ZnO/PANI photocatalytic degradation of the metronidazole (MNZ) at various radiation times was investigated under UV as well as visible light radiation [50]. The authors reported that at neutral pH (*viz.* pH = 7.0), both type of radiations (UV and visible light) showed 100% removal of the MNZ after 3 h radiation. However, at basic medium (pH = 10.0), the removal percentage of MNZ in both radiations were found to be 88% and 86%, respectively. A better adsorption of MNZ at pH 7.0 is attributed to a hydrogen bond and  $\pi$ - $\pi$  interaction with the ZnO/PANI nanocomposite and MNZ. As explained earlier in this section, other factors that were reported to affect the photocatalytic activity include the type of the nanoparticle used and the type of polymer as a host material.

Özbay et al. [52] reported on the photocatalytic activity of polyaniline/ZnO for the photodegradation of Sunfix red S3B reactive dye. The authors investigated the influence of the irradiation time, photocatalyst, and dye concentration. It was noticed that the increase in dye concentration and photocatalyst dosage increased the removal efficiency due to a large number of active sites that increased the number of available hydroxyl radicals. The optimal dosage was found to be 1.6 g/L. The irradiation period of 10 min was sufficient for the degradation of the dye, regardless of the dye concentration. In their work, Eskizeybek and coworkers reported that the PANI/ZnO nanocomposite exhibited high photodegradation efficiency for methylene blue (MB) and malachite green (MG) under sunlight and UV light irradiation [53]. The photocatalytic performance under sunlight radiation was higher when compared to UV-light radiation. The degradation efficiency for both dyes was found to increase with an increase in photocatalyst dosage until 0.4 mg/mL,

after which the efficiency was stable. This was attributed to a large surface area, which allows for the exposure of active sites available for photocatalytic reactions. The availability of these active sites may increase with the increase in photocatalyst content, but the light penetration was reduced due to a smaller surface area resulting from aggregation as well as light scattering. The photocatalytic efficiency of 99% for both dyes under natural sunlight was attained after 5 h. The efficiency of the photocatalyst under UV-light irradiation was ~95% for MB and ~98% for MG after 10 h. The material maintained higher photocatalytic efficiency after five repeated cycles, indicating the reusability of the resultant composites.

A thin coating layer of PANI on ZnO was obtained by mixing ZnO with dedoped PANI followed by filtration and drying at 60 °C [54]. It was reported that the maximum photocatalytic efficacy for ampicillin was achieved under sunlight irradiation when the irradiation period was 2 h, at a pH value of 5, and the initial ampicillin concentration of 4.5 mg/L. It can be deduced that a combination of ZnO with conductive polymers facilitates the photocatalytic efficiency of pollutants because of the strong interaction between these polymers and ZnO, which contribute to more electrons to the conduction band of ZnO. On the other hand, experimental conditions such as pH, concentration of the pollutant, and photocatalyst dosage are important to achieve the desired photocatalytic results. The studies on the effect of ZnO content on the photocatalytic behavior of conductive polymers are scarce, hence, more studies are required to give an overview of the resulting degradation performance. It can be estimated that the higher content of ZnO within the host conductive polymer can positively increase the overall degradation performance because more of the particles will be exposed. Nonetheless, Saravanan et al. [55] studied the influence of PANI concentration on the photocatalytic behavior of the nanocomposites. The authors kept the ZnO content at 1.0 g while varying the ratio of PANI (i.e., 1, 1.5, 2 M) in the polymerization solution. The BET surface area increased with an increase in the PANI ratio, but the TEM images deduced that at high PANI content, there was significant agglomeration of the nanoparticles. The latter was ascribed to strong intermolecular interaction between ZnO and PANI. The band gap was, however, reported to decrease with an increase in the PANI content. The maximum photocatalytic performance was attained for 1.5 M PANI with a MO degradation of ~98% and MB degradation of ~99% within 2 h. In addition, the composite exhibited good stability and reusability for the photodegradation of dye after three cycles, suggesting its applicability in wastewater remediation. The efficiency of 1.5 M PANI-based composites was attributed to high crystallinity and strong intermolecular interaction between ZnO and PANI without noticeable agglomeration. When comparing the photocatalytic efficiency of a non-conductive polymer in the form of PMMA with the conductive polymers' systems, it was realized that the conductive polymer showed higher photocatalytic efficiencies. For example, Mauro et al. [56] reported on the photocatalysis of the ZnO/PMMA by low-temperature atomic layer deposition. The nanocomposites were fabricated by three various methods: (i) atomic layer deposition (ALD) of ZnO on PMMA and Si plates; (ii) atomic layer deposition of ZnO PMMA and solution; and (iii) sonication and solution casting. The photocatalytic activity of the nanocomposites was tested against two organic pollutants in water (i.e., methylene blue (MB) dye and sodium lauryl sulfate (SDS), an anionic surfactant). The morphology of the ZnO/PMMA fabricated by the ALD revealed that ZnO covered the PMMA, while the ALD + solution casting revealed the presence of voids, and the solution casting method showed holes in the PMMA matrix in which the ZnO embedded itself into those holes. The samples were subjected to UV light irradiation for the photocatalytic activity of MB. All the samples showed a reasonable efficacy in terms of the degradation of the MB dye. To be specific, the degradation of MB was reported to be approximately 62%, 55%, and 67% for ZnO "ALD", ZnO "ALD + solution casting", and ZnO solution casting, respectively. The difference in degradation % of MB was associated with the varied nanostructures of the samples. The SDS degradation was conducted for 4 h under UV light. The degradation of SDS was reported to be 64% (ZnO "ALD"), 66% (ZnO "ALD + solution casting"), and 73% (solution casting). When comparing the degradation of the two pollutants, the SDS pollutants were

more degraded when compared with the MB. The behavior is associated with the positive charge of the ZnO, which enhances the interaction with the anionic surfactant, whereas the interaction is hindered with MB, which is positively charged.

#### 4.2. Synergistic Effect of the ZnO with Other Nanoparticles Reinforced Polymer Composites

There have been a few studies [57–60] that have investigated the morphology and photocatalytic activity of ZnO with other nanoparticles incorporated into the polymer matrices. The synergy of the nanoparticles is expected to show better efficiency when compared with ZnO alone. Furthermore, the synergy of ZnO with other nanoparticles is important since ZnO undergoes easy self-oxidation when exposed to UV irradiation, in the process reducing the photocatalytic activity. In order to solve such a problem, ZnO is paired with another filler in order to avoid self-oxidation and improve the photostability of the overall composites. Naji et al. [57] reported on the photocatalytic degradation of methylene blue by the ZnO–Ag/polystyrene and ZnO/polystyrene systems. The ZnO–Ag synergy was fabricated by the photo deposition, and the ZnO–Ag/PS composite film was prepared by solution mixing using chloroform as a solvent. The photocatalytic activity of the ZnO–Ag/PS as well as ZnO/PS composites were analyzed by the degradation of methylene under a UV lamp. The synergy of ZnO–Ag within the polystyrene was found to be effective in terms of enhancing the photodegradation of methylene blue when compared with the ZnO-PS. According to the UV–Vis spectra (Figure 8), the MB was realized to have a maximum absorption at 665 nm, with the absorption at this peak being monitored to investigate the extent of MB degradation. Both ZnO–Ag/PS and ZnO–Ag/PS composites reduced the MB absorption gradually with time until the color changed due to the photocatalytic reaction. According to Figure 8d, the photodegradation efficiency of the samples is as follows: (i) 97% for ZnO–Ag/PS; (ii) 70% efficiency for ZnO/PS; and (iii) PS alone was found to be 19%. The main reason the ZnO–Ag/PS was found to be more effective in photocatalytic degradation was due to the presence of more active sites in the presence of Ag in the ZnO–Ag/PS composite.

The very same samples (i.e., (a) ZnO/PS composite, and (b) ZnO–Ag/PS film) were investigated for photodegradation after being reused three times. The aim of re-using the catalysts after they underwent three lots of photodegradation was to prove that the catalysts are cost-effective. This is beneficial in ensuring that there is a reduction in terms of the consumption of the catalyst. The efficiency of photodegradation was found to be 89% for ZnO–Ag/PS, while the ZnO/PS film reached an efficiency of 76%. In some cases, semiconductor quantum dots were incorporated into the synergistic system in order to enhance the photocatalytic properties. Iqbal and co-workers [58] reported on the photodegradation of the mesoporous TiO<sub>2</sub> in synergy with the ZnO quantum dots incorporated in the linear low polyethylene (LLDPE). The composites were fabricated by the solution casting for photodegradation of the tetracycline (TC) antibiotics through the fluorescent light irradiation. The composite was prepared by incorporating 8% of the TiO<sub>2</sub>/ZnO-quantum (TZ) into the LLDPE matrix. The morphology of the ZT incorporated into the LLDPE was undertaken by transmission electron microscopy (TEM). The neat nanoparticles of ZnO QDs and ZT were found to be irregular and spherical, accompanied by agglomeration (Figure 9). The average particle sizes for ZT and ZnO QDs were reported to be  $12.5 \pm 2.05$  nm and  $4.12 \pm 0.23$  nm, respectively.

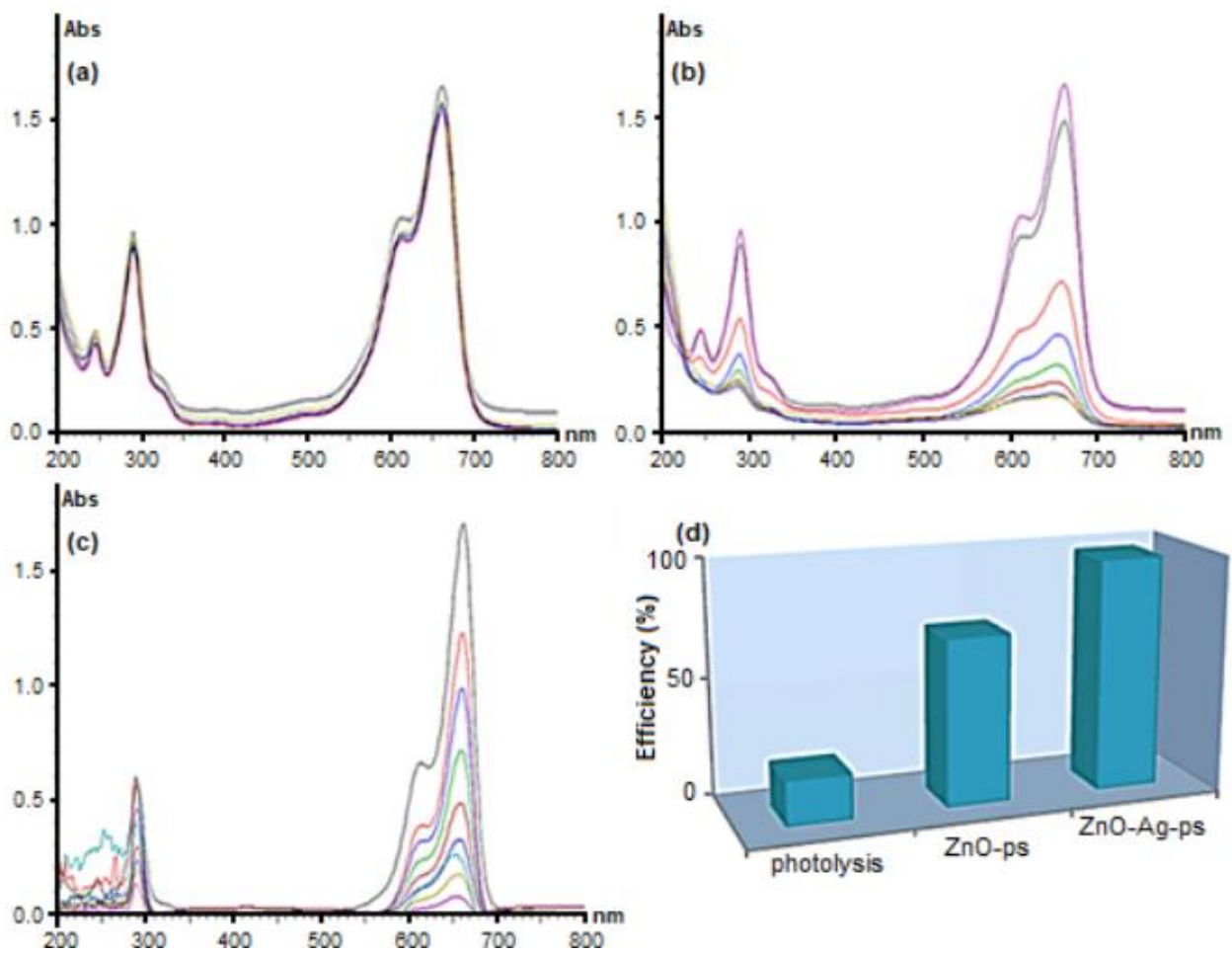


**Figure 8.** Photodegradation activity of methylene blue (MB). (a) PS sample, (b) ZnO/PS composite, (c) ZnO-Ag/PS film, and (d) efficiency of photodegradation. Reprinted from [57].

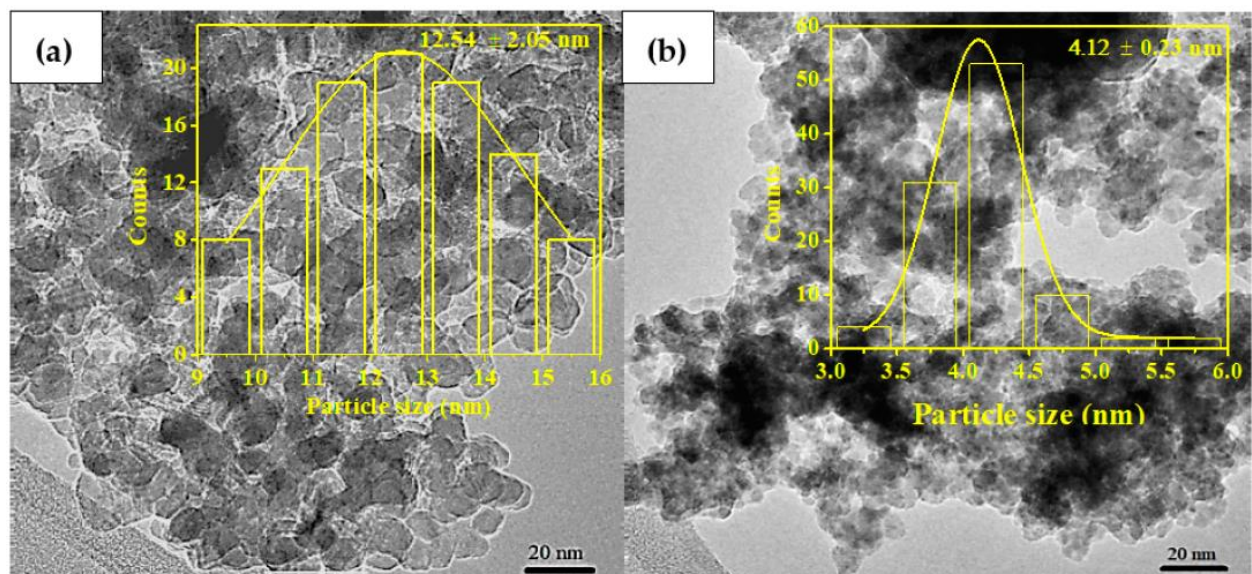


**Figure 9.** TEM samples of the (a) neat ZT and (b) ZnO QD. The average particles are represented by the insert. Reprinted from [58].

According to the FESEM, ZT was found to have pores and the average pore diameter was reported to be  $1.17\ \mu\text{m}$  (Figure 10). The reason for pores was attributed to the utilization of starch during the synthesis of the nanoparticles. The cross-sectional image of the 8%ZT@LLDPE (Figure 10d) was reported to be free of microcracks and voids.

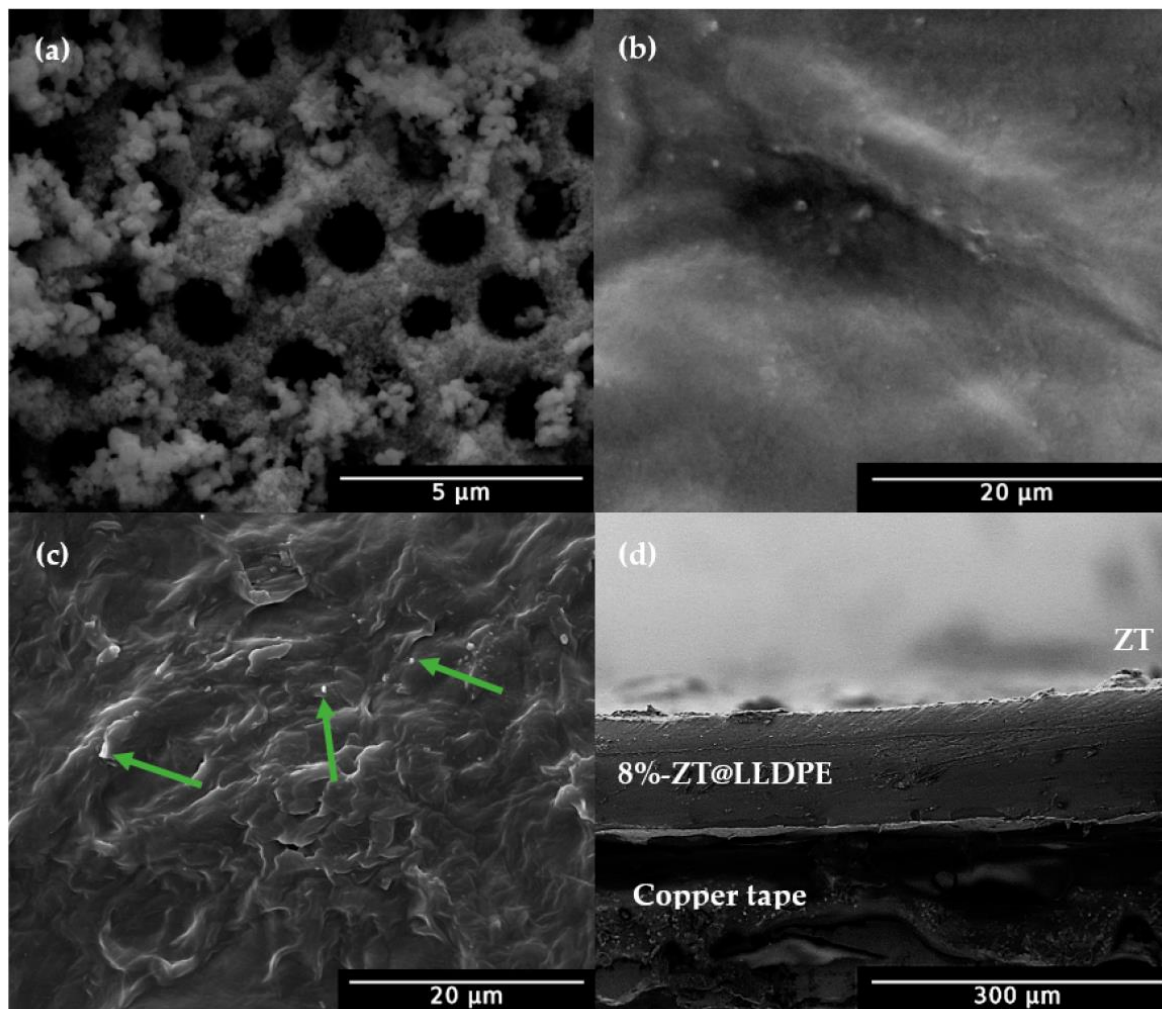


**Figure 10.** FESEM images of (a) ZT, (b) neat LLDPE, (c) 8%-ZT@LLDPE, and (d) cross-section of the 8%-ZT@LLDPE nanocomposite positioned on the film without any visible microcracks or voids. Green arrows indicate white spots representing ZnO QDs. Reprinted from [58].

The  $\text{TiO}_2$ /LLDPE composite removed 42.7% of the tetracycline (TC) while the zinc oxide quantum was found to be effective when compared with  $\text{TiO}_2$ , with the ZnO QD revealing a 53.4% removal of tetracycline (TC). This might be due to the generation of more reactive sites for ZnO QDs than the  $\text{TiO}_2$ . The 8%ZT/LLDPE composite resulted in the highest efficiency removal of 85.4%. This was associated with the designation of the heterojunction between the nanofillers (*viz.* ZnO QDs and  $\text{TiO}_2$ ), which results in separation of the photogenerated  $e^-/h^+$  pairs. The mineralization efficiency and reusability of the composites after photodegradation were reported. There was an enhancement in the mineralization efficiency with an increase in time. The 8%-TZ@LLDPE system was found to have a higher mineralization efficiency (Figure 11a) than both the neat LLDPE and P25@LLDPE. For neat LLDPE, low mineralization efficiency was expected since there was no catalyst. The high efficiency in the presence of both semiconductive nanofillers was attributed to the formation of an effective heterojunction between the nanofillers, which most probably allows for the separation of the  $e^-/h^+$ , which in turn improves the recombination rate for photocatalytic activity. Similarly, the reusability is very important

in photocatalysis since it provides more information on the photostability. Since the 8%-TZ@LLDPE system was found to be effective in terms of the photocatalytic degradation of the tetracycline (TC), it was chosen for the analysis of reusability wherein the sample was subjected to eight cycles of photodegradation. According to Figure 11b, the sample exhibited a comparable degradation efficiency after eight cycles, which supports the idea that this system may be stable enough for potential use in photocatalyst film applications.

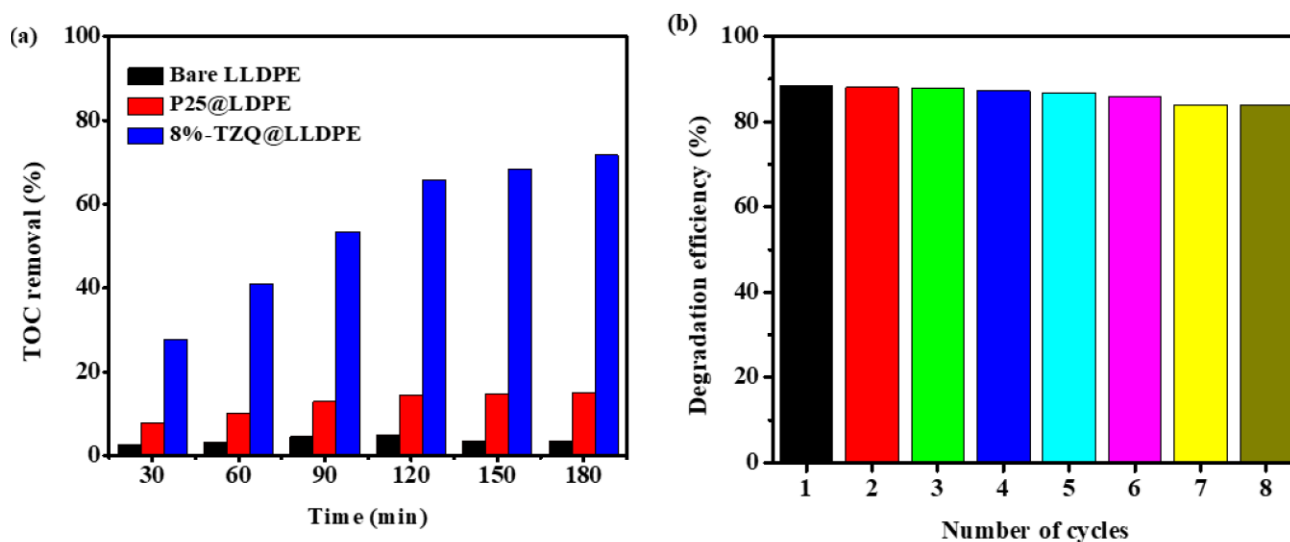
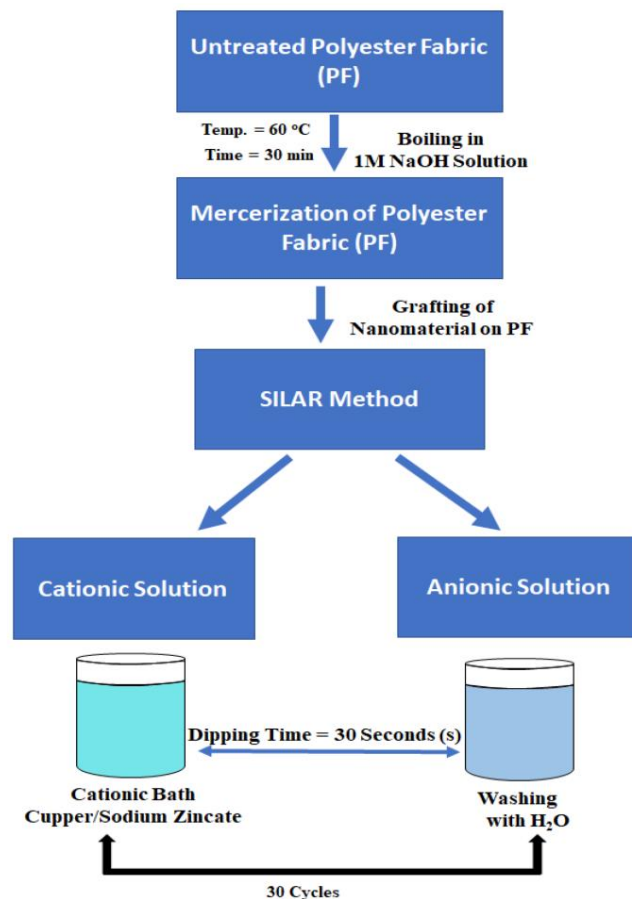


**Figure 11.** (a) Photocatalytic mineralization of TC for neat LLDPE and its hybrid system, and (b) recycled experiments utilizing 8%-TZ@LLDPE. Reprinted from [58].

ZnO and CuO were grafted into the polyester membrane to improve the photocatalytic reduction of Cr(VI). The reason Cr(IV) was investigated is because it is a toxic heavy metal, as a result, there is a need for its removal in wastewater. Scheme 1 illustrates the various steps for fabrication of the ZnO/CuO nanocomposite into the polyester [59]. The SEM images of the ZnO/CuO/polyester nanocomposite revealed that the polyester fabric was covered with flake-nanostructures. The reason for such a dense covering of the nanoparticles into the polyester fabric was associated with the alkaline treatment of the fabric, which produced roughness on the surface. It is generally known that in most cases, a rough surface is able to produce reaction sites for the ease of penetration by other materials, in this case, the nanoparticles. As a reference point, the concentration of Cr(VI) was measured by UV-Vis spectroscopy and recorded to be 200 ppm. The inserted test tubes in Figure 12 shows the wastewater before treatment (yellow test tube) and after treatment (clear test tube). The yellow color in the other container indicated the presence of Cr(VI), while the clear color indicated that the solar photocatalytic reduction reduced the concentration Cr(VI) in wastewater. According to Figure 12, it became evident that the continuous exposure of pure wastewater to irradiation reduced the concentration of Cr(VI) in water. For example, at 0 h, the concentration was approximately 200 ppm, while after 6 h, the concentration was found to be 24 ppm.

A ternary system composed of ZnO/ reduced graphene oxide (rGO)/PANI was prepared to evaluate the synergy among the components on the photocatalytic performance of nanocomposites toward methyl orange (MO) under UV-light irradiation [61]. The ternary composite composed of ZnO/rGO/PANI was prepared via the in situ chemical oxidative polymerization of aniline. It was found that rGO was decorated with ZnO particles and both were wrapped with PANI sheets. The increase in PANI in the system decreased the photocatalytic efficiency of the composites. The maximum MO photodegradation efficiency of ~99% under UV-light was attained within an hour. Such an improvements resulted from PANI providing dye adsorption sites, allowing light penetration, and increasing the separation efficacy of the photogenerated electron-hole pairs. However, the excessive PANI

content formed a thick layer aggregating on the surface of ZnO, thus blocking the light and migration of excited electrons from the PANI layer to the encapsulated ZnO particles. The composites maintained high photodegradation efficiency even after three cycles, indicating its reusability and stability.



Scheme 1. Various steps of grafting ZnO/CuO into the polyester. Reprinted from [59].

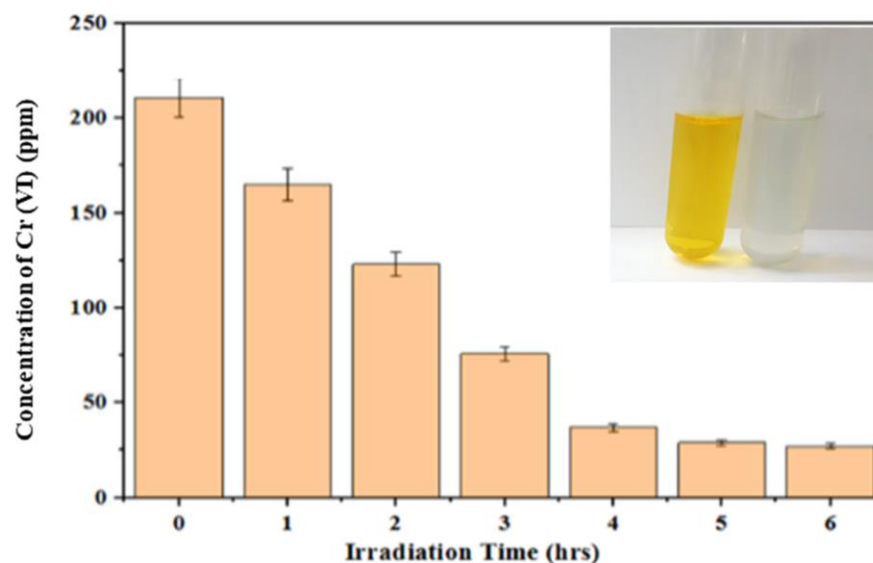


Figure 12. Irradiation time vs. concentration of the Cr(VI) for ZnO/CuO/PMR (inserted image indicate real wastewater before (yellow coloured solution) and after treatment (a clear solution)). Reprinted from [59].

Since the recovery of the photocatalyst is one essential factor from the ecological and economic viewpoints, the decoration of ZnO with magnetic particles for their recovery using an external magnet was demonstrated by Zhang et al. [62]. The authors prepared PANI-Fe<sub>3</sub>O<sub>4</sub>@ZnO core-shell microsphere photocatalysts using Pickering emulsion one-step synthesis. Spherical microspheres with diameters of ~1.5 μm displayed high magnetization to afford their separation using an external magnet. With a BET surface area of ~11.2 m<sup>2</sup>/g, the as-prepared microspheres showed high photocatalytic activity. The highest MB photocatalytic degradation efficiency of ~91% was achieved within 40 min under visible light irradiation. A recent study by Neda et al. [63] demonstrated that the Fe<sub>3</sub>O<sub>4</sub>/ZnO/PANI core-shell structure can be prepared by encapsulating Fe<sub>3</sub>O<sub>4</sub> with ZnO followed by the in situ polymerization of PANI as a host matrix. In this case, Fe<sub>3</sub>O<sub>4</sub> nanoparticles were synthesized separately and then dropped into a zinc acetate dehydrate solution to afford the synthesis of ZnO as a shell. Subsequently, PANI synthesis using aniline was carried out in the presence of the as-prepared core-shell nanoparticles. Spherical particles with diameters ranging in between 35 and 50 nm with a magnetization of ~20 emu/g were obtained. It was noticed that Congo red (CR) decomposition reached 81% within 15 min under visible light at the photocatalyst dosage of 2.0 g/L and initial dye concentration of 60 g/L. The maximum photodegradation pH value was ~3 with 86% CR decomposition after 15 min. The decomposition of (CR) increased with an increase in temperature and the composites showed 7.3% reduction after five repeated cycles, whereas Fe<sub>3</sub>O<sub>4</sub>/ZnO had 14.8%. The Ag/ZnO/PMMA nanocomposite was fabricated for the degradation of organic pollutants such as methylene blue, sodium lauryl sulfate, and paracetamol [64]. The addition of Ag into the ZnO/PMMA nanocomposites facilitated a 30% enhancement in the photocatalytic capacity of MB when compared with PMMA/ZnO. According to the authors, this behavior was associated with a delayed recombination time of the charge carriers by the metal. The Ag/ZnO/PMMA nanocomposites was also reported to have 65% improvement in the photocatalytic degradation of paracetamol when compared with the ZnO/PMMA nanocomposite. There was more than 90% in the degradation of SDS in the presence of the Ag/ZnO/PMMA nanocomposite. The presence of Ag enhanced the photocatalytic activity of the ZnO/PMMA nanocomposites due to the ability of the Ag to act as an electron sink, decreasing the possibility of the electron-hole recombination and promoting an effective charge separation.

## 5. Conclusions and Future Recommendations

The limitations in the availability of fresh water and continuous water pollution have prompted researchers to invest more time in various methods for the treatment of water. The source of polluted water is attributed to the pollutants (i.e., oils, organic solvents, dyes, etc.) produced by industries due to their evolution. The photocatalytic activity was found to be very efficient in terms of the removal of pollutants. ZnO has been identified as one of the most effective photocatalysts in the process of photocatalytic degradation due to its wide bandgap (*viz.* 3.37 eV), low cost, and thermal stability. Factors such as the dispersion of ZnO within the polymer matrix, type of ZnO (i.e., nanorods, spheres, and nanowires), synergy with other nanoparticles, pH, and preparation method were reported to have an effect on the photocatalytic activity of the ZnO/polymer composites. The use of preparation methods that can result in more photocatalytic fillers being exposed is of essence to reduce the time required while maintaining a high degradation efficiency. On the other hand, experimental conditions such as pH, concentration of the pollutant, and photocatalyst dosage are important to achieve the desired photocatalytic results. In general, the use of conventional non-conductive polymers as host materials can negatively affect the photocatalytic behavior of ZnO particles. With most of these systems resulting in a degradation efficacy of less than 70%, this is a major concern from an economic viewpoint. In addition, this type of composite takes longer to achieve the desired degradation efficiency. The use of conductive polymers could even further improve the photocatalytic efficiency of the resultant composites [49]. These polymers are known to act as a sensitizer to

promote the spectrum response of inorganic semiconductors within the visible light region. Up to now, conductive polymers can be regarded as the best polymer systems when incorporated with a photocatalyst, since higher photocatalytic activity has been reported in such systems and photocatalytic efficiency has been reported to be as high as 99%. The synergy of ZnO with other photocatalysts such as Ag and TiO<sub>2</sub> were found to be effective in terms of photocatalytic degradation, with an efficiency as high as 89% in some cases due to the presence of more reactive sites in the synergy of nanoparticles. For future purposes, it would be very interesting if more work is conducted on the polymer blends as host matrices for ZnO in the process of photocatalytic degradation, as this may widen the applications of ZnO. It would be interesting to report on the molecular weight and resultant properties of the polymer blends/ZnO nanocomposites after being exposed to UV irradiation. Another suggestion for future purposes would be the utilization of ZnO with more than two photocatalysts, since it has been observed that the utilization of ZnO with another nanoparticle enhances the photocatalytic degradation more.

**Funding:** This research was co-funded by Department of Science and Innovation-National Research Foundation (NRF-DSI) and National Research Foundation (NRF).

**Conflicts of Interest:** The authors declare no conflict of interest.

## References

1. Manisalidis, I.; Stavropoulou, E.; Bezirtzoglou, E. Environmental and health impacts of air pollution. A review. *Front. Public Health* **2020**, *8*, 14. [[CrossRef](#)]
2. Li, J.; Yang, J.; Liu, M.; Ma, Z.; Fang, W.; Bi, J. Quality matters: Pollution exacerbates water scarcity and sectoral output risks China. *Water Res.* **2022**, *224*, 119059.
3. Wang, L.; Zhang, J.; Wei, J.; Zong, J.; Lu, C.; Du, Y.; Wang, Q. Association of ambient air pollution exposure and its variability with subjective sleep quality in China: A multilevel modeling analysis. *Environ. Pollut.* **2022**, *312*, 120020. [[CrossRef](#)] [[PubMed](#)]
4. Hossain, E.; Faruque, H.M.R.; Sunny, M.d.S.H.; Mohammad, N.; Nawar, N. A comprehensive review on energy storage systems: Types, comparison, current scenario, applications barriers, and potential solutions policies, and future prospects. *Energy* **2020**, *13*, 3651. [[CrossRef](#)]
5. Gössling, S.; Meyer-Habighorst, C.; Humpe, A. A global review of marine air pollution policies, their scope and effectiveness. *Ocean Coast. Manag.* **2021**, *212*, 105824. [[CrossRef](#)]
6. Jadoun, S.; Yáñez, J.; Mansilla, H.D.; Riaz, U.; Chauhan, N.P.S. Conducting polymers/zinc oxide-based photocatalysts for environmental remediation: A review. *Environ. Chem. Lett.* **2022**, *20*, 2063–2083. [[CrossRef](#)] [[PubMed](#)]
7. Haq, A.U.; Saeed, M.; Khan, S.G.; Ibrahim, M. Photocatalytic applications of titanium dioxide (TiO<sub>2</sub>). In *Titanium Dioxide-Advances and Applications*; Ali, H.M., Ed.; Intech Open: London, UK, 2021. [[CrossRef](#)]
8. Khulbe, K.C.; Matsuura, T. Removal of heavy metals and pollutants by membrane adsorption techniques. *Appl. Water Sci.* **2018**, *8*, 19. [[CrossRef](#)]
9. Shabangu, K.P.; Bakare, B.F.; Bwapwa, J.K. The treatment of chemical coagulation process in South African brewery wastewater: Comparison of polyamine and aluminium-chlorohydrate coagulants. *Water* **2022**, *14*, 2495. [[CrossRef](#)]
10. Rubi, H.; Fall, C.; Ortega, R.E. Pollutant removal from oily wastewater discharged from car washes through sedimentation-coagulation. *Water Sci. Technol.* **2009**, *59*, 2359–2369. [[CrossRef](#)]
11. El-Baz, A.A.; Hendy, I.A.; Dohdoh, A.M.; Srour, M.I. Adsorption technique for pollutants removal; current new trends and future challenges—a review. *Egypt. J. Eng. Sci. Technol.* **2020**, *32*, 1–24. [[CrossRef](#)]
12. Muruganandam, L.; Kumar, M.P.S.; Jena, A.; Gulla, S.; Godhwani, B. Treatment of water by coagulation and flocculation using biomaterials. *IOP Conf. Ser. Mater. Sci. Eng.* **2017**, *263*, 032006. [[CrossRef](#)]
13. Ren, G.; Han, H.; Wang, Y.; Liu, S.; Zhao, J.; Meng, X.; Li, Z. Recent advances of photocatalytic application in water treatment: A review. *Nanomaterials* **2021**, *11*, 1804. [[CrossRef](#)]
14. Schneider, J.; Matsuoka, M.; Takeuchi, M.; Zhang, J.; Horiuchi, Y.; Anpo, M.; Bahnemann, D.W. Understanding TiO<sub>2</sub> photocatalysis: Mechanisms and materials. *Chem. Rev.* **2014**, *114*, 9919–9986. [[CrossRef](#)]
15. Nakata, K.; Fujishima, A. TiO<sub>2</sub> photocatalysis: Design and applications. *J. Photochem. Photobiol. C* **2012**, *13*, 169–189. [[CrossRef](#)]
16. Nur, H.; Misnon, I.I.; Wei, L.K. Stannic oxide-titanium dioxide coupled semiconductor photocatalyst loaded with polyaniline for enhanced photocatalytic oxidation of 1-octene. *Int. J. Photoenergy* **2007**, *2007*, 098548. [[CrossRef](#)]
17. Uddin, M.d.T.; Hoque, M.d.E.; Bhoomick, M.C. Facile one-pot synthesis of heterostructure SnO<sub>2</sub>/ZnO photocatalyst for enhanced photocatalytic degradation of organic dye. *RSC Adv.* **2020**, *10*, 23554–23565. [[CrossRef](#)]
18. Lin, Z.; Du, C.; Yan, B.; Yang, G. Amorphous Fe<sub>2</sub>O<sub>3</sub> for photocatalytic hydrogen evolution. *Catal. Sci. Technol.* **2019**, *9*, 5582–5592.
19. Minhas, P.S.; Saha, J.K.; Dotaniya, M.L.; Sarkar, A.; Saha, M. Wastewater irrigation in India: Current status, impacts and response options. *Sci. Total Environ.* **2022**, *808*, 152001. [[CrossRef](#)]

20. Xu, L.; Hu, Y.-L.; Pelligra, C.; Chen, C.-H.; Jin, L.; Huang, H.; Sithambaram, S.; Aindow, M.; Joesten, R.; Suib, S.L. ZnO with different morphologies synthesized by solvothermal methods for enhanced photocatalytic activity. *Chem. Mater.* **2009**, *21*, 2875–2885. [[CrossRef](#)]
21. Nadzim, U.K.H.M.; Hairom, N.H.H.; Hamdan, M.A.H.; Ahmad, M.K.; Jalil, A.A.; Jusoh, N.W.C.; Hamzah, S. Effects of different zinc oxide morphologies on photocatalytic desulfurization of thiophene. *J. Alloys Compd.* **2022**, *913*, 165145. [[CrossRef](#)]
22. Furka, D.; Furka, S.; Naftaly, M.; Rakovský, E.; Čaplovičová, M.; Janek, M. ZnO nanoparticles as photodegradation agent controlled by morphology and boron doping. *Catal. Sci. Technol.* **2021**, *11*, 2167–2185. [[CrossRef](#)]
23. Prabakaran, E.; Pillay, K. Synthesis of N-doped nanoparticles with cabbage morphology as a catalyst for the efficient photocatalytic degradation of methylene blue under UV and visible light. *RSC Adv.* **2019**, *9*, 7509–7535. [[CrossRef](#)] [[PubMed](#)]
24. Kasumov, A.M.; Korotkov, K.A.; Karavaeva, V.M.; Zahornyi, M.M.; Dmitriev, A.I.; Levtyushenko, A.I. Photocatalysis with the use of ZnO nanostructures as a method for the purification of aquatic environments from dyes. *J. Water Chem. Technol.* **2021**, *43*, 281–288. [[CrossRef](#)]
25. Ardila-Leal, L.D.; Poutou-Piñales, R.A.; Pedroza-Rodríguez, A.M.; Quevedo-Hidalgo, B.E. A brief history of colour, the environmental impact of synthetic dyes and removal by using. *Molecules* **2021**, *26*, 3813. [[CrossRef](#)] [[PubMed](#)]
26. Du, Y.; Xu, X.; Liu, Q.; Bai, L.; Hang, K.; Wang, D. Identification of organic pollutants with potential ecological and health risks in aquatic environments: Progress and challenges. *Sci. Total Environ.* **2022**, *806*, 150691. [[CrossRef](#)]
27. Liu, X.; Wang, G.; Zhi, H.; Dong, J.; Hao, J.; Zhang, X.; Wang, J.; Li, D.; Liu, B. Synthesis of the porous ZnO nanosheets and TiO<sub>2</sub>/ZnO/FTO composite films by a low-temperature hydrothermal method and their applications in photocatalysis and electrochromism. *Coatings* **2022**, *12*, 695. [[CrossRef](#)]
28. Serpone, N.; Emeline, A.V.; Horikoshi, S.; Kuznetsov, V.N.; Ryabchuk, V.K. On the genesis of heterogenous photocatalysis: A brief historical perspective in the period 1910 to the mid-1980s. *Photochem. Photobiol. Sci.* **2012**, *11*, 1121–1150. [[CrossRef](#)]
29. Teichner, S.J. The origins of photocatalysis. *J. Porous Mater.* **2008**, *15*, 311–314. [[CrossRef](#)]
30. Keidel, E. The fading of aniline dyes in the presence of titanium white. *Farben-Ztg.* **1929**, *34*, 1242–1243.
31. Goodeve, C.F.; Kitchener, J.A. The mechanism of photosensitization by solids. *Trans. Faraday Soc.* **1938**, *34*, 902–912. [[CrossRef](#)]
32. Kato, S.; Mashio, F. *Book of Abstracts of the 9th Annual Meeting of the Chemical Society of Japan*; American Association for the Advancement of Science: Kyoto, Japan, 1956; p. 223.
33. Fujishima, A.; Honda, K. Electrochemical photolysis of water at a semiconductor electrode. *Nature* **1972**, *238*, 37–38. [[CrossRef](#)] [[PubMed](#)]
34. Kato, K.; Masuo, F. Liquid-phase oxidation of tetralin using titanium oxide as a photocatalyst. *Kogyo Kagaku Zasshi* **1964**, *67*, 1136–1140. [[CrossRef](#)]
35. Bakbolai, B.; Daulbayev, C.; Sultanov, F.; Beissenov, R.; Umirzakov, A.; Mereke, A.; Bekbaev, A.; Chuprakov, I. Recent development of TiO<sub>2</sub>-based photocatalysis in the hydrogen evolution and photodegradation: A review. *Nanomaterials* **2020**, *10*, 1790. [[CrossRef](#)]
36. Ng, K.H. Adoption of TiO<sub>2</sub>-photocatalysis for palm oil mill effluent (POME) treatment.: Strengths, weaknesses, opportunities, threats (SWOT) and its practicality against traditional treatment in Malaysia. *Chemosphere* **2021**, *270*, 129378. [[CrossRef](#)] [[PubMed](#)]
37. Arcanjo, G.S.; Mounteer, A.H.; Bellato, C.R.; Da Silva, L.M.M.; Dias, S.H.B.; Da Silva, P.R. Heterogenous photocatalysis using TiO<sub>2</sub> modified with hydrotalcite and iron oxide under UV-visible irradiation for color and toxicity reduction in secondary textile mill effluent. *J. Environ. Manage.* **2018**, *211*, 154–163. [[CrossRef](#)]
38. Guo, C.; Wang, K.; Hou, S.; Wan, L.; Lv, J.; Zhang, Y.; Qu, X.; Chen, S.; Xu, J. H<sub>2</sub>O<sub>2</sub> and TiO<sub>2</sub> photocatalysis under UV irradiation for the removal of antibiotic resistant bacteria and their antibiotic resistance genes. *J. Hazard. Mater.* **2017**, *323*, 710–718. [[CrossRef](#)]
39. Okuno, T.; Kawamura, G.; Muto, H.; Matsunda, A. Fabrication of shape-controlled Au nanoparticles in a TiO<sub>2</sub>-containing mesoporous template using UV irradiation and their shape-dependent photocatalysis. *J. Mater. Sci. Technol.* **2014**, *30*, 8–12. [[CrossRef](#)]
40. Bendjabeur, S.; Zoughi, R.; Zouchoune, B.; Sehili, T. DFT and TD-DFT insights, photolysis and photocatalysis investigation of three dyes with similar structure under UV irradiation with and without TiO<sub>2</sub> as a catalyst: Effect of adsorption, pH and light intensity. *Spectrochim. Acta A Mol. Biomol. Spectrosc.* **2018**, *190*, 494–505. [[CrossRef](#)]
41. Nur, A.S.M.; Sultana, M.; Mondal, A.; Islam, S.; Robel, F.N.; Islam, A.; Sumi, M.S.A. A review on the development of elemental and codoped TiO<sub>2</sub> photocatalysts for enhanced dye degradation under UV-vis irradiation. *J. Water Process. Eng.* **2022**, *47*, 102728. [[CrossRef](#)]
42. Sharma, P.; Hasan, M.R.; Mehto, N.K.; Deepak; Bishoyi, A.; Narang, J. 92 years of zinc oxide: Has been studied by the scientific community since the 1930s-an overview. *Sens. Int.* **2022**, *3*, 100182. [[CrossRef](#)]
43. Lea, M.C. On allotropic forms of silver. *Am. J. Sci.* **1889**, *37*, 476–491. [[CrossRef](#)]
44. Paal, C. Über colloidalen Silber. *Dtsch. Z. Chir.* **1921**, *163*, 62–84.
45. Moudry, Z.V. Process of Producing Oligodynamic Metal Biocides. United States Patent 2, 927,052, 20 March 1953.
46. Qiu, R.; Zhang, D.; Mo, Y.; Song, L.; Brewer, E.; Huang, X.; Xiong, Y. Photocatalytic activity of polymer-modified ZnO under visible light irradiation. *J. Hazard. Mater.* **2008**, *156*, 80–85. [[CrossRef](#)]
47. Kamalian, P.; Khorasani, S.N.; Abdolmaleki, A.; Karevan, M.; Khalili, S.; Shirani, M.; Neisiany, R.E. Toward the development of polyethylene photocatalytic degradation. Toward the development of polyethylene photocatalytic degradation. *J. Polym. Eng.* **2020**, *40*, 181–191. [[CrossRef](#)]

48. Prasert, A.; Sontikaew, S.; Sriprapai, D.; Chuangchote, S. Polypropylene/ZnO nanocomposites: Mechanical properties, photocatalytic dye degradation, and antibacterial property. *Materials* **2020**, *13*, 914. [[CrossRef](#)]
49. Asgari, E.; Esrafil, A.; Jafari, A.J.; Kalantary, R.R.; Noumoradi, H.; Farzadkia, M. The comparison of ZnO/polyaniline nanocomposite under UV and visible radiations for decomposition of metronidazole: Degradation rate, mechanism and mineralization. *Process Saf. Environ. Prot.* **2019**, *128*, 65–76. [[CrossRef](#)]
50. Colmenares, J.C.; Kuna, E.; Jakubiak, S.; Michalski, J.; Kurzydłowski, K. Polypropylene nonwoven filter with nanosized ZnO rods: Promising hybrid photocatalyst for water purification. *Appl. Catal. B* **2015**, *170–171*, 273–282. [[CrossRef](#)]
51. Tofa, T.S.; Kunjali, K.L.; Paul, S.; Dutta, J. Visible light photocatalytic degradation of microplastic residues with zinc oxide nanorods. *Environ. Chem. Lett.* **2019**, *17*, 1341–1346. [[CrossRef](#)]
52. Özbay, B.; Genç, N.; Bağhaki, B.; Zor, S. Photocatalytic activities of polyaniline-modified TiO<sub>2</sub> and ZnO under visible light: An experimental and modeling study. *Clean Technol. Environ. Policy.* **2016**, *18*, 2591–2601. [[CrossRef](#)]
53. Eskizeybek, V.; Sari, F.; Gülce, H.; Gülce, A.; Avci, A. Preparation of the new polyaniline/ZnO nanocomposite and its photocatalytic activity for degradation of methylene blue and malachite green dyes under UV and natural sun lights irradiations. *Appl. Catal. B* **2012**, *119–120*, 197–206. [[CrossRef](#)]
54. Olad, A.; Nosrati, R. Use of response surface methodology for optimization of the photocatalytic degradation of ampicillin by ZnO/polyaniline nanocomposite. *Res. Chem. Intermed.* **2015**, *41*, 1351–1363. [[CrossRef](#)]
55. Saravanan, R.; Sacari, E.; Gracia, F.; Khan, M.M.; Mosquera, E.; Gupta, V.K. Conducting PANI stimulated ZnO system for visible light photocatalytic degradation of coloured dyes. *J. Mol. Liq.* **2016**, *221*, 1029–1033. [[CrossRef](#)]
56. Di Mauro, A.; Farrugia, C.; Abela, S.; Refalo, P.; Grech, M.; Falqui, L.; Privitera, V.; Impellizzeri, G. Synthesis of ZnO/PMMA nanocomposite by low-temperature atomic layer deposition for possible photocatalysis applications. *Mater. Sci. Semicond. Process.* **2020**, *118*, 105214. [[CrossRef](#)]
57. Naji, H.K.; Oda, A.M.; Abduljaleel, W.; Abdilkadhim, H.; Hefdh, R. ZnO-Ag/PS and ZnO/PS films for photocatalytic degradation of methylene blue. *Indones. J. Chem.* **2020**, *20*, 314–323. [[CrossRef](#)]
58. Iqbal, A.; Saidu, U.; Adam, F.; Sreekantan, S.; Yahaya, N.; Ahmad, M.N.; Ramalingam, R.J.; Wilson, L.D. Floating ZnO QDs-modified TiO<sub>2</sub>/LLDPE hybrid polymer film for the effective photodegradation of tetracycline under fluorescent light irradiation: Synthesis and characterization. *Molecules* **2021**, *26*, 2509. [[CrossRef](#)]
59. Ashar, A.; Bhatti, I.A.; Jilani, A.; Mohsin, M.; Rasul, S.; Iqbal, J.; Shakoor, M.B.; Al-Sehemi, A.G.; Wageh, S.; Al-Ghamdi, A.A. Enhanced solar photocatalytic reduction of Cr(VI) using a (ZnO/CuO) nanocomposite grafted onto a polyester membrane for wastewater treatment. *Polymers* **2021**, *13*, 4047. [[CrossRef](#)]
60. Lam, S.-M.; Sin, J.-C.; Zeng, H.; Lin, H.; Li, H.; Li, H.; Chai, Y.-Y.; Choong, M.-K.; Mohamed, A.R. Green synthesis of Fe-ZnO nanoparticles with improved sunlight photocatalytic performance for polyethylene film deterioration and bacterial inactivation. *Mater. Sci. Semicond.* **2021**, *123*, 105574. [[CrossRef](#)]
61. Wu, H.; Lin, S.; Chen, C.; Liang, W.; Liu, X.; Yang, H. A new ZnO/rGO/polyaniline ternary nanocomposite as photocatalyst with improved photocatalytic activity. *Mater. Res. Bull.* **2016**, *83*, 434–441. [[CrossRef](#)]
62. Zhang, X.; Wu, J.; Meng, G.; Guo, X.; Liu, C.; Liu, Z. One-step synthesis of novel PANI-Fe<sub>3</sub>O<sub>4</sub>@ZnO core-shell microspheres: An efficient photocatalyst under visible light irradiation. *Appl. Surf. Sci.* **2016**, *366*, 486–493. [[CrossRef](#)]
63. Zare, N.; Kojoori, R.K.; Abdolmohammadi, S.; Sadegh-Samiei, S. Ultrasonic-assisted synthesis of highly effective visible light Fe<sub>3</sub>O<sub>4</sub>/ZnO/PANI nanocomposite: Thoroughly kinetics and thermodynamic investigations on the Congo red dye decomposition. *J. Mol. Struct.* **2022**, *1250*, 131903. [[CrossRef](#)]
64. Di Mauro, A.; Farrugia, C.; Abela, S.; Refalo, P.; Grech, M.; Falqui, L.; Nicotra, G.; Sfuncia, G.; Mio, A.; Buccheri, M.A.; et al. Ag/ZnO/PMMA nanocomposites for efficient water reuse. *ACS Appl. Bio Mater.* **2020**, *3*, 4417–4426. [[CrossRef](#)] [[PubMed](#)]